Sains Malaysiana 45(5)(2016): 833–839

Production and Characterization of the Defatted Oil Palm Shell Nanoparticles

(Penghasilan dan Pencirian Nanopartikel Tempurung Kelapa Sawit Ternyah Lemak)

ABDUL KHALIL, H.P.S.*, MD. SOHRAB HOSSAIN, NUR AMIRANAJWA, A.S., NURUL FAZITA, M.R., MOHAMAD HAAFIZ, M.K., SURAYA, N.L.M., DUNGANI, R. & FIZREE, H.M.

ABSTRACT

This present study was conducted to produce defatted oil palm shell (OPS) nanoparticles. Wherein, the OPS nanoparticles were defatted by solvent extraction method. Several analytical methods including transmission electron microscope (TEM), X-ray diffraction (XRD), particle size analyzer, scanning electron microscope (SEM), SEM energy dispersive X-ray (SEM-EDX) and thermal gravimetric analyzer (TGA) were used to characterize the untreated and defatted OPS nanoparticles. It was found that 75.3% OPS particles were converted into nanoparticles during ball milling. The obtained OPS nanoparticles had smaller surface area with angular, irregular and crushed shapes under SEM view. The defatted OPS nanoparticles did not show any agglomeration during TEM observation. However, the untreated OPS nanoparticles had higher decomposition temperature as compared to the defatted OPS nanoparticles. Based on the characterization results of the OPS nanoparticles, it is evident that the defatted OPS nanoparticles has the potentiality to be used as filler in biocomposites.

Keywords: Composite materials; nanofiller; nanoparticles; oil extraction; oil palm shell; solvent extraction

ABSTRAK

Kajian ini telah dijalankan untuk menghasil dan mencirikan partikel nano tempurung kelapa sawit (OPS) yang telah dinyahlemak. Partikel nano OPS telah dinyahlemak melalui kaedah pengestrakan pelarut. Beberapa kaedah analisis termasuk mikroskop elektron pancaran (TEM), pembelauan sinar-X (XRD), penganalisis saiz partikel, mikroskop elektron imbasan (SEM), SEM sinar-X serakan tenaga (SEM-EDX) dan penganalisis gravimetrik terma (TGA) telah digunakan untuk mencirikan partikel nano OPS yang tidak dirawat dan yang telah dinyahlemak. Didapati bahawa 75.3% daripada partikel OPS telah ditukarkan kepada partikel nano semasa proses pengisaran bola. Partikel nano OPS yang diperoleh menerusi pengimejan SEM mempunyai kawasan permukaan yang lebih kecil dengan bersudut, tidak teratur dan berbentuk hancur. Partikel nano OPS yang dinyahlemak tidak menunjukkan sebarang pengumpulan semasa pemerhatian TEM. Walau bagaimanapun, partikel nano OPS yang tidak dirawat mempunyai suhu penguraian yang lebih tinggi berbanding dengan partikel nano OPS yang dinyahlemak. Berdasarkan keputusan pencirian partikel nano OPS, adalah jelas bahawa partikel nano OPS yang dinyahlemak mempunyai potensi untuk digunakan sebagai pengisi dalam komposit bio.

Kata kunci: Bahan komposit; partikel nano; pengekstrakan minyak; pengekstrakan pelarut; pengisi nano; tempurung kelapa sawit

INTRODUCTION

Malaysia is the second largest palm oil producer country in the world. Palm oil industry in Malaysia is generating large volume of industrial waste as a by-product in the form of empty fruit bunch, mesocarp fibre and oil palm shell (OPS). The amount waste generation is increasing with increasing number of palm oil industries and palm plantation in Malaysia. It was being reported that Malaysia produces about 4 million tons OPS annually (Abdul Khalil et al. 2011). This OPS waste material caused environmental pollution and requires high financial investment for disposing (Abdul Khalil et al. 2011; Gobi & Vadivelu 2013; MPOC 2012). Some of the oil palm industries used these OPS waste materials as fuel for boiler. The utilization of OPS as boiler fuel created serious emission problem in palm oil industry (Chow & Ho 2002). It appears that palm oil mill boiler emits the emission over the permissible limit (0.4 g Nm^{-3}) set by the Department of Environment of Malaysia (Md Kawser & Farid Nasir 2000). In order to preserve the environment, scientists have taken initiative to utilize OPS into various useful materials such as activated carbon, adsorbent for the removal of gases from air pollutants, as well as for filler in composites (Abdul Khalil et al. 2010; Arami-Niya et al. 2010; Hussien et al. 2011; Lua et al. 2001).

In recent years, the emphasis on sustainable materials has increased. The growing demand for sustainable development motivated researchers to define the application of industrial waste materials as fillers in composite or concrete materials (Abdullah et al. 2010; Foo & Hameed 2010). However, the OPS, is an industrial by-products that have received attention to be used as

fillers due to its potential characteristics including low cost, abundance, renewability and sustainability (Abdullah et al. 2010; Foo & Hameed 2010; Report-TH 2013). Therefore, the incorporation OPS waste as nano fillers in the form of particulate fillers into composites in place of mineral fillers such as calcium carbonate, mica and talc would be an economical approach. However, the presence of small amount of oil in the OPS might reduce the properties of the end products and restricts its application for advanced composites engineering (Bi et al. 2008). The trace amount of residual oil in OPS affects the mechanical properties of natural fiber reinforced composites due to the increased in interactions between the oil molecules and the polymer chains of the matrix (Ngo et al. 2013). These chemical interactions weakened the polymer crosslinking network thus led to early failure of the material.

Several methods can be used to remove the residual oil from the OPS including mechanical pressing (MPOB 2013), including supercritical fluid extraction and solvent extraction (Ferreira-Dias et al. 2003; Liauw et al. 2008). However, solvent extraction is a widely used method, offers some distinct advantages over other methods including higher yield, lower operating cost and easy to operate (Ogunleye et al. 2012). Therefore, the present study was conducted in order to produce nanoparticles from OPS. The residual oil present in OPS was extracted by solvent extraction method using n-hexane as solvent. Further, the properties of the oil free OPS nanoparticles were characterize using various analytical methods and compared with the untreated OPS nanoparticles.

Materials and Methods

Preparation of the OPS nanoparticles

Oil palm shells (OPS) chips were collected from a palm-oil processing mill in PT. Kertajaya Banten, Indonesia in the form of chips. The OPS chips were ground in a Willey mill to become granular particles. The ground OPS particles were dried at 110°C for 24 h to minimize the moisture content into 1.5%. Subsequently, it was further ground using a grinder/refiner followed by high-energy ball milling for 30 h at 170 rev min^{-1} with a ratio of balls to powder of 10:1 (Abdul Khalil et al. 2011). The ground sample were then dried in an oven at 105°C for 2 h and then placed in desiccators prior to further analysis.

Extraction of residual oil from OPS nanoparticles

OPS nanoparticles were undergone extraction with n-hexane by a Soxtec™ 2043 (Foss, Denmark) for removing residual oil. About 50 g of OPS nanoparticle was placed into the thimble and inserted in an soxhlet extraction unit, connected to a reaction flask containing 250 mL of n-hexane. The extraction was conducted at 75°C for 90 min (Ferreira-Dias et al. 2003). The defatted sample were dried in oven at 105°C for 12 h and placed in desiccators before analysis.

Analysis of OPS nanoparticles

Particle size distribution of OPS was assessed by a MALVERN Zetasizer Ver. 6.11 (MAL 1029406, Germany) with dynamic light scattering measurements set at 532 nm laser. The experiments were carried out triplicate to ensure the accuracy of the results. For transmission electron microscopy (TEM) analysis, 0.5 mg samples were put in distilled water and dispersed with an ultrasonicator for 10 min. A drop of colloidal dispersion containing OPS was placed onto a carbon-coated copper grid before being examined under the TEM (Philips CM12).

X-ray diffraction (XRD) analysis was carried out with a Philips PW1050 X-pert diffractometer using Cu-Ka1 radiation at 40kV, 25Ma and $\lambda = 1.54$ Å. The diffractrograms were scanned from 2 to 90° (2θ) with a step of 0.05° at a scanning rate of 0.5° min^{-1} at room temperature. The X-ray diffraction (XRD) analysis was conducted to determine the particle size and crystallinity of OPS nanoparticles.

Scanning electron microscopy (SEM) was used to characterize the morphology of the OPS nanoparticles after gold coating with an iron sputter coater (Polaron SC515, Fisons Instruments, UK). A SEM (LEO Supra 50 Vp, Germany) was used for particle surface as well as surface texture analysis. The SEM analysis was extended to obtain the elemental composition of the OPS nanoparticles by means of energy dispersive X-ray analysis (SEM-EDX). A Perkin Elmer thermal gravimetric analyzer (TGA-6) was used to investigate the thermal decomposition of the OPS nanoparticles from 30 to 800°C under nitrogen environment at a heating rate of 20°C/min.

Results and Discussion

Solvent extraction of the residual oil from OPS nanoparticles showed a trace amount of oil in OPS. Approximately, 1.6% palm oil was extracted from OPS nanoparticles using n-hexane at 75°C for 90 min (data not shown). Figure 1 shows the particle size distribution of OPS nanoparticles by intensity which covers wide range of particles with symmetric behavior of curve. However, the diameter of the major portion of the particle ranged between 50.8 to 91.3 nm, which covers 75% of the nanoparticles. Thus, the result confirmed that the particles were in nano size (Koo 2006). These particle size variations were developed during ball milling process. Similarly results were also reported by Dungani et al. (2013).

Figure 2 shows the untreated and defatted OPS nanoparticles by soxhlet extraction. The rough surface in Figure 2(a) proves the presence of residual palm oil in untreated OPS nanoparticles. From this Figure 2(a), it can be assumed that the diameter of the oil molecules is bigger than the OPS nanoparticles. These oil molecules were tremendously stable and did not fuse to form a homogenous layer after separation. This stability is because of a layer of surface active agents covering the surface of the oil molecules (Chow & Ho 2002). These oil molecules gave

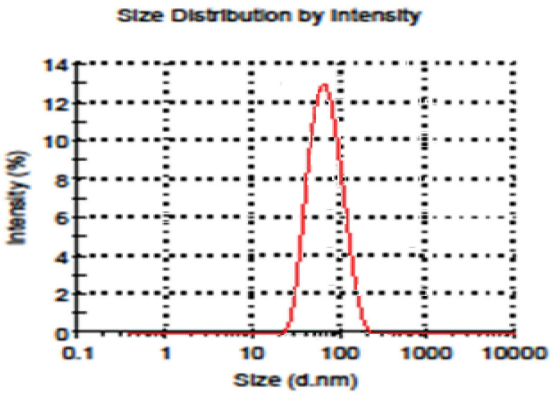

FIGURE 1. Particle size distribution of defatted OPS nanoparticles

poor interfacial adhesion when untreated OPS nanoparticles were added into any matrices. Additionally, oil molecules significantly increased the biodegradability of natural fiber reinforced composites (Ngo et al. 2013). The clear and smooth surface of treated OPS nanoparticles TEM image in Figure 2(b) showed that the n-hexane successfully removed the oil present in OPS nanoparticles.

The size of the OPS nanoparticles ranges between 10 and 30 nm having irregular circular shapes by SEM analysis, indicating their nanometric nature. The study also confirms that there was no agglomeration of OPS nanoparticles after the extraction. The average crystallite size was determined from X-ray diffraction peaks using Scherrer's equation (Patterson 1939).

$$D = \frac{K\lambda}{\beta \cos\theta}, \tag{1}$$

where D is the crystallite diameter; λ is the X-Ray wavelength; β is the full width at half maximum of the diffraction peak; θ is the diffraction angle; and K is the Scherrer's constant of the order of unity for usual crystals. As shown in Figure 3, the reflecting peak at 2θ = 20.31°, 21.15° and 22.15° were used to estimate the size of the OPS nanoparticles resulting the particle size of 44.46, 29.19 and 21.61 nm, respectively. The average size of OPS nanoparticles was 31.75 nm.

The crystallinity index (CI) of OPS nanoparticles was calculated using the peak deconvolution method of XRD intensity data. Following (2) where CI is calculated from the ratio of the area of all crystalline peaks (A_{Cr}) to the

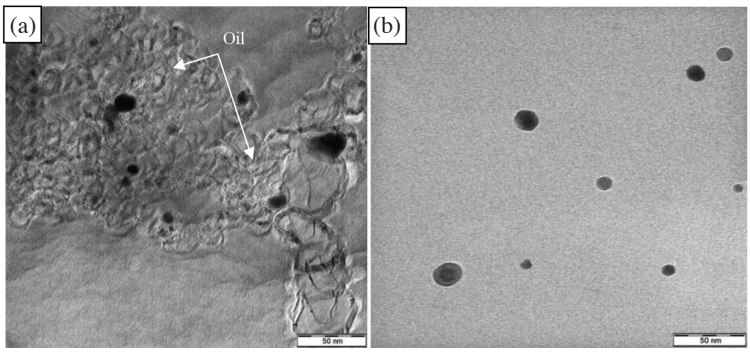

FIGURE 2. TEM micrographs of OPS nanoparticles.a: untreated; and b: defatted

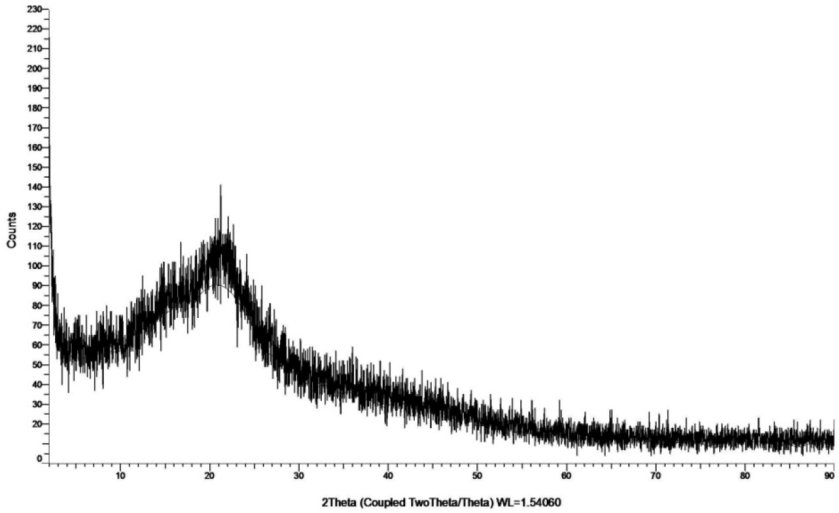

FIGURE 3. XRD spectrum of defatted OPS nanoparticles

total area (A_{total}), the CI of OPS nanoparticle was found to be 15.2%.

$$CI = \frac{A_{Cr}}{A_{total}} \times 100. \quad (2)$$

Dungani et al. (2013) found similar level of crystallinity index for OPS nanoparticles. The index had significant influence on hardness, density, transparency and diffusion of the end products. These changes in the crystallographic pattern of cellulose were observed due to damage of the crystalline structures of cellulose samples during milling and hence decreased the crystallinity. XRD diffraction analysis indicated that the crystallinity of nano-structured material from OPS decreased as the particle size decreased. This result consistent with the result reported by Paul et al. (2007), who reported that high energy ball milling decrease the size of particle together with crystallinity of the nanoparticles.

Figure 4(a) shows the SEM photomicrographs of OPS particle before been subjected to high-energy ball milling. While Figure 4(b) and 4(c), shows the morphology of untreated and defatted OPS nanoparticles. The structure of OPS broke down and the particle size reduced to nanoscale with ball milling time Paul et al. (2007). SEM micrograph showed that the OPS nanoparticles became angular, irregular and crushed shapes subjected to high energy ball milling process. There was no significant change of the surface morphology between untreated and defatted OPS nanoparticles. Hence, the solvent extraction of residual from OPS nanoparticles using n-hexane did not alter the surface morphology of OPS. Along with the solid spheres, irregularly shaped particle of OPS nanoparticles can be seen which are larger in size due to the agglomeration of nanoparticles on the SEM morphology analysis. This agglomerated sphere and irregularly shaped amorphous particle can also be detected which may be because of the inter-particle fusion during the sample analysis. Thus, it was not possible to detect a single particle even at higher magnifications using SEM analysis which might be related to the agglomeration of the nanoparticles and restricted of SEM analysis itself.

SEM equipped with energy dispersive X-ray analysis (SEM-EDX) was used to determine the chemical constituents of OPS nanoparticles. Figure 5 shows the EDX spectrum of untreated (Figure 5(a)) and defatted (Figure 5(b)) OPS nanoparticles. Table 1 presents the elemental weight (%) obtained from EDX analysis. Both OPS nanoparticles showed the presence of carbon, oxygen, sodium, chlorine and indium, Wan Daud and Ali (2004) reported the presence of carbon and oxygen with similar percentage in the raw OPS. However, the results might vary due to the particle size, particle fabrication method and variety of the oil palm shells. Table 1 shows that the weight of carbon, chlorine and indium decrease after the oil extraction, while oxygen and sodium increase. Qualitatively, this variation might be because of the removal of oil from the OPS nanoparticles. Palm oil mostly contains palmitic acid ($C_{16}H_{32}O_2$) and oleic acid ($C_{18}H_{34}O_2$) acid, therefore these organic constitute extracted by hexane during the solvent

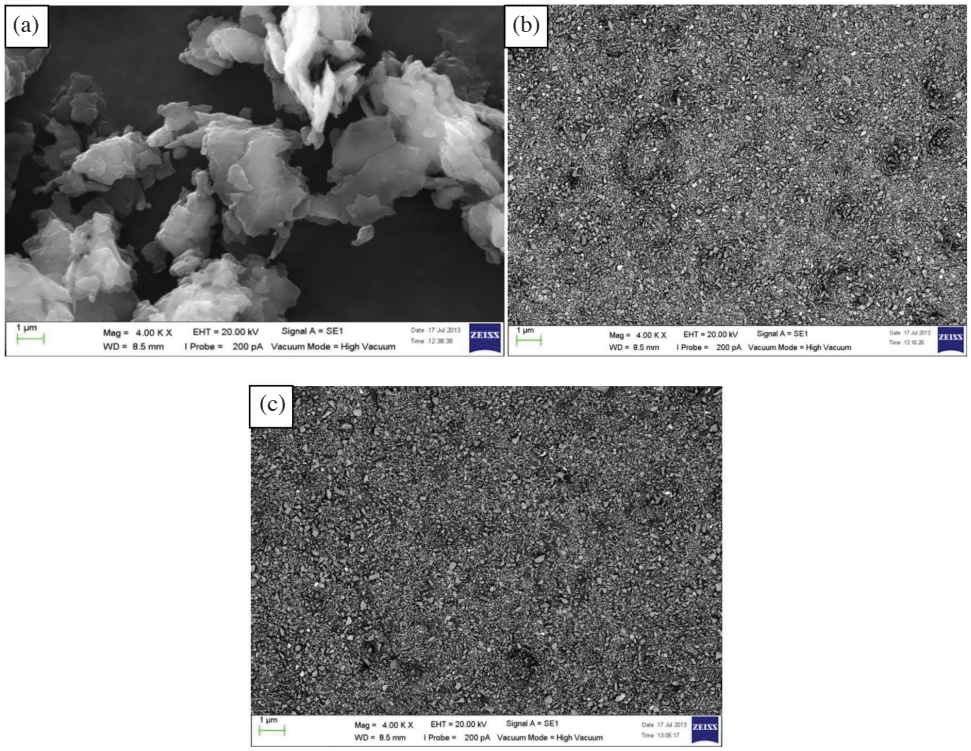

FIGURE 4. The SEM photomicrographs of (a) OPS particle, (b) untreated OPS nanoparticles and (c) Defatted OPS nanoparticles

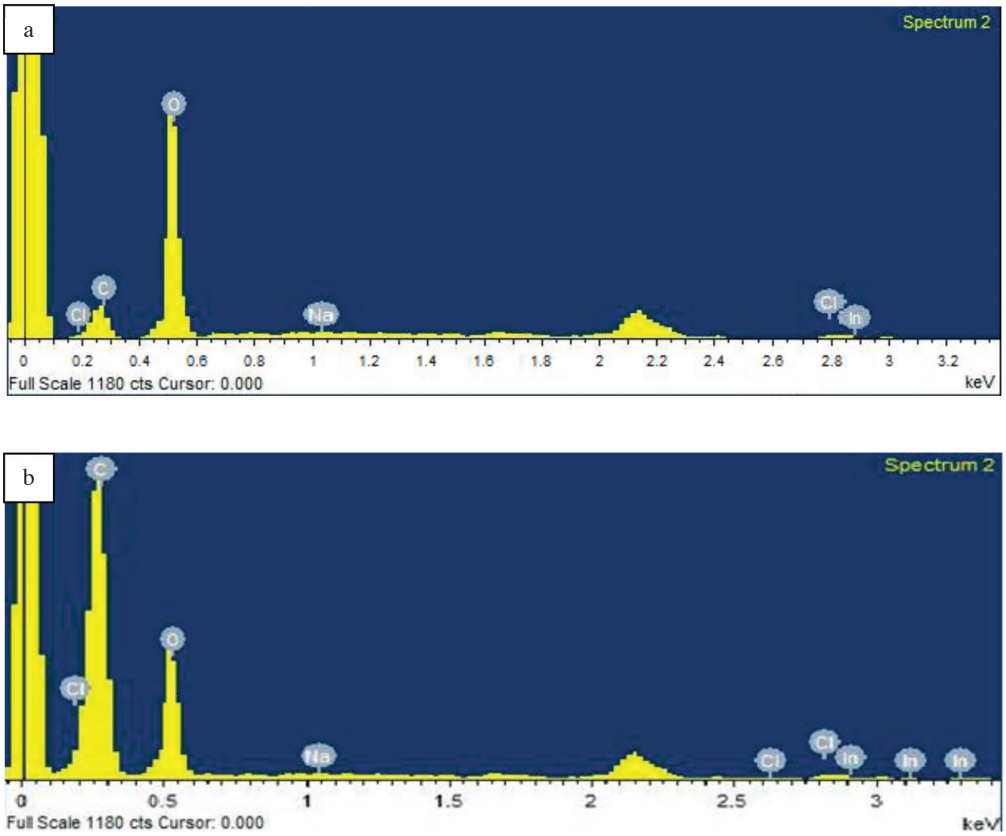

FIGURE 5. SEM-EDX analysis of (a) untreated and (b) defatted OPS nanoparticles

TABLE 1. Percentage elemental composition of OPS nanoparticles

Elemental	Untreated OPS nanoparticles		Defatted OPS nanoparticles	
	Weight%	Atomic%	Weight%	Atomic%
C K	67.47	67.96	43.69	51.64
O K	43.04	29.99	53.43	47.41
Na K	0.15	0.09	0.89	0.55
Cl K	3.07	1.20	0.56	0.22
In L	6.26	0.76	1.43	0.18
Totals	100	-	100	-

extraction of residual oil from OPS nano particles (MPOB 2013).

Figure 6 shows the TGA curves of untreated and defatted OPS nanoparticles. The extracted curve shows a slight weight loss before 100°C which corresponds to the evaporation of moisture from the particles, while the un-extracted OPS nanoparticles shows a gradually weight loss up to 300°C. This is called the first stage of decomposition which usually corresponds to the drying phase where light volatiles and water removes from the particles. In the second stage of decomposition at temperature between 200 and 800°C or initial decomposition temperature (T_i) of OPS nanoparticles, weight progressively drops due to the liberation of volatile hydrocarbon from thermal decomposition of cellulose, hemicelluloses and some part of lignin. Table 2 shows the summarized result of thermal properties of untreated and defatted OPS nanoparticles determined from DTG curve from TGA analysis (not shown). The untreated OPS nanoparticles have higher decomposition temperature (582°C) compared to the extracted nanoparticles (278°C). This might be because of the presence of oil in the un-extracted nanoparticles. According to Gaur and Reed (1998), hemicelluloses decompose at 200 to 350°C due to its linear polymer structure with short side chains. Whereas, cellulose decomposes at 305 to 375°C and lignin gradually over at 250 to 500°C (Abdullah et al. 2010).

Wan Nik et al. (2005) reported that the pure palm oil decomposition temperature 347°C, adding some additives managed to protect the oil from oxidation thus increase the decomposition temperature. The higher decomposition temperature of un-extracted OPS

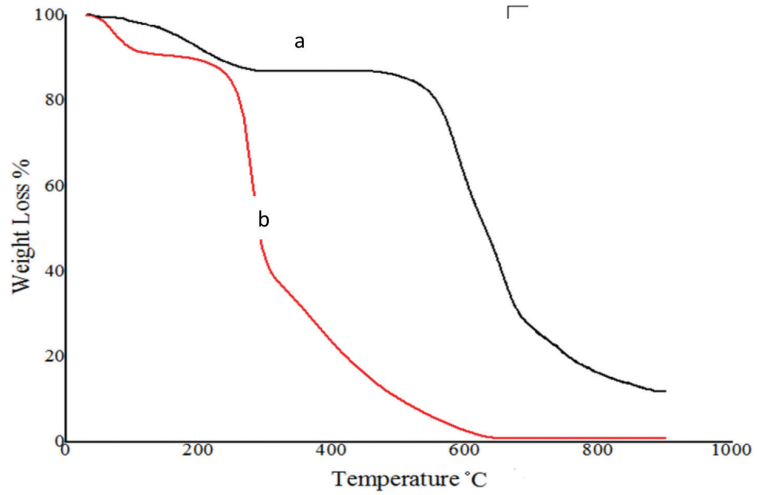

FIGURE 6. Thermogravimetric analysis of OPS nanoparticles (a) Untreated and (b) Defatted

TABLE 2. Thermal parameters for thermograms of OPS nanoparticles

OPS	Degradation Temperature (°C)			Char Residue (%)	DTG peak
	T_i	T_f	$T_{50\%}$		T_{max} (°C)
Untreated	582	698	656	12.42	642
Defatted	278	401	308	1.68	297

nanoparticles could be because of the oil itself which the nanoparticles also manage to protect the oil from oxidation. Hence, the presence of oil enhances thermal stability of the OPS nanoparticles. After the degradation, all the volatile materials were driven off from the sample resulting in the residual char or ash content of 17.8 and 2.2% for untreated and defatted OPS nanoparticles, respectively. The untreated OPS nanoparticles contains higher fixed-carbon content due to the presence of oil and thereby, it was more difficult to degrade and result in higher residual char or ash content.

CONCLUSION

Extraction of residual oil from OPS nanoparticles showed that solvent extraction using n-hexane as solvent effectively removed the oil. The average diameter of the OPS nanoparticles was within the range 50.75 to 91.28 nm. Particle formation of defatted OPS nanoparticles showed the absence of uniformity with size distribution intensity of 75.30%. XRD analysis showed that the particles size of the defatted OPS nanoparticles within the range 21.61 to 44.46 nm. The shape and surface of the defatted OPS nanoparticles were angular, irregular and crushed shapes. SEM analysis showed that the shape, surface texture and composition element of the OPS nanoparticles has changed during the ball milling process. The defatted OPS nanoparticle exhibited lower degree of crystallinity with higher amorphous area compare to untreated OPS nanoparticles. From the result, the trace amount of residual oil in OPS nanoparticles was successfully removed, thus the incorporation of this material with polymer matrix can improve polymer crosslinking network. Hence, it was evident that the defatted OPS nanoparticles can be used as filler in biocomposites.

ACKNOWLEDGEMENTS

The authors would like to thank the Ministry of Education (MOE), Malaysia for providing the Research grant as financial support, Grant. No. FRGS-203 / PTEKIND / 6711325.

REFERENCES

Abdul Khalil, H.P.S., Fizree, H., Jawaid, M. & Alattas, O.S. 2011. Preparation and characterization of nano structured materials from oil palm ash: a bio-agricultural waste from oil palm mill. *BioResources* 6(4): 4537-4546.

Abdul Khalil, H.P S., Poh, B.T., Jawaid, M., Ridzuan, R., Suriana, R., Said, M.R., Ahmad, F. & Nik Fuad, N.A. 2010. The effect of soil burial degradation of oil palm trunk fiber-filled recycled polypropylene composites. *J. Reinf. Plast. Compos.* 29(11): 1653-1663.

Abdullah, S., Yusup, S., Ahmad, M.M., Ramli, A. & Ismail, L. 2010. Thermogravimetry study on pyrolysis of various lignocellulosic biomass for potential hydrogen production. *Cellulose* 20: 42-20.

Arami-Niya, A., Wan Daud, W.M.A. & Mjalli, F.S. 2010. Using granular activated carbon prepared from oil palm shell by $ZnCl_2$ and physical activation for methane adsorption. *J. Anal. Appl. Pyrolysis* 89(2): 197-203.

Bi, Y., Luo, R., Li, J., Feng, Z. & Jin, Z. 2008. The effects of the hydraulic oil on mechanical and tribological properties of C/C composites. *Mat. Sci. Eng*. A 483: 274-276.

Chow, M. & Ho, C. 2002. Chemical composition of oil droplets from palm oil mill sludge. *J. Oil Palm Res*. 14: 25-34.

Dungani, R., Islam, M.N., Abdul Khalil, H.P.S. Hartati, S., Abdullah, C.K., Dewi, M. & Hadiyane, A. 2013. Termite resistance study of oil palm trunk lumber (OPTL) impregnated with oil palm shell meal and phenol- formaldehyde resin. *BioResources* 8(4): 4937-4950.

Ferreira-Dias, S., Valente, D.G. & Abreu, J.M. 2003. Comparison between ethanol and hexane for oil extraction from Quercus suber L. fruits. *Grasas y Aceites* 54(4): 378-383.

Foo, K. & Hameed, B. 2010. Insight into the applications of palm oil mill effluent: a renewable utilization of the industrial agricultural waste. *Renew. Sustainable Energy Rev.* 14(5): 1445-1452.

Gaur, S. & Reed, T.B. 1998. Thermal data for natural and synthetic fuels. CRC Press.

Gobi, K. & Vadivelu, V. 2013. By-products of palm oil mill effluent treatment plant–A step towards sustainability. *Renew. Sustainable Energy Rev.* 28: 788-803.

Hussein, M.Z.B., Abdul Rahman, M.B.B., Yahaya, A.H., Hin, T.-Y.Y. & Ahmad, N. 2001. Oil palm trunk as a raw material for activated carbon production. *J. Porous Mat*. 8(4): 327-334.

Koo, J.H. 2006. *Polymer Nanocomposites: Processing, Characterization, and Applications*. New York: McGraw-Hill.

Liauw, M. Y., Natan, F., Widiyanti, P., Ikasari, D., Indraswati, N., & Soetaredjo, F. 2008. Extraction of neem oil (*Azadirachta indica* A. Juss) using n-hexane and ethanol: studies of oil quality, kinetic and thermodynamic. *ARPN J. Eng. Appl. Sci*. 3(3): 49-54.

Lua, A.C. & Guo, J. 2001. Microporous oil-palm-shell activated carbon prepared by physical activation for gas-phase adsorption. *Langmuir* 17(22): 7112-7117.

Md Kawser, J. & Farid Nasir, A. 2000. Oil palm shell as a source of phenol. *J. Oil Palm Res*. 12: 86-94.

MPOB. 2013. Malaysia: Malaysian Palm Oil Board. Malaysian Palm Oil Industry [Online].

MPOC. 2012. Malaysian Palm Oil Industry. Available at: http://www.mpoc.org.my/Malaysian_Palm_Oil_Industry.aspx.

Ngo, T.T., Lambert, C.A., Bliznyuk, M. & Kohl, J.G. 2013. Effect of a tertiary oil phase on the mechanical properties of natural fiber-reinforced polyester composites. *Polym-Plast Technol*. 52(11): 1160-1168.

Ogunleye, O. & Eletta, O. 2012. Nonlinear programming for solvent extraction of *Jatropha curcas* seed oil for biodesiel production. *Int. J Energy Eng*. 2(2): 8-14.

Patterson, A.L. 1939. The Scherrer formula for x-ray particle size determination. *Phys. Rev.* 56(10): 978.

Paul, K., Satphaty, S., Manna, I., Chakraborty, K. & Nando, G. 2007. Preparation and characterization of nano structured materials from fly ash: a waste from thermal power stations by high energy ball milling. *Nano Res Lett* 2(8): 397 - 404.

Report-TH. 2013. Palm Oil Production Comparison.

Singh, G., KimHuan, L., Leng, T. & Kow, D.L. 1999. *Oil Palm and the Environment: A Malaysian Perspective*. Malaysian Oil Palm Growers' Council.

Wan Daud, W.M.A. & Ali, W.S.W. 2004. Comparison on pore development of activated carbon produced from palm shell and coconut shell. *Bioresour. Technol*. 93(1): 63-69.

Wan Nik, W., Ani, F.N. & Masjuki, H. 2005. Thermal stability evaluation of palm oil as energy transport media. *Energy Conv. Manag*. 46(13): 2198-2215.

Abdul Khalil, H.P.S.*, Md. Sohrab Hossain, Nur Amiranajwa, A.S.,Nurul Fazita, M.R., Mohamad Haafiz, M.K., Suraya, N.L.M. & Fizree, H.M.
School of Industrial Technology
Universiti Sains Malaysia
11800 Penang
Malaysia

Dungani, R.
School of Life Sciences and Technology
Institut Teknologi Bandung
Gedung Labtex XI, Jalan Ganesha 10
Bandung 40132, West Java
Indonesia

*Corresponding author; email: mfizree@gmail.com

Received: 3 April 2015
Accepted: 2 December 2015